

Supplementary Information

Ultratrace level detection of Cu²⁺ in aqueous medium by novel Zn(II)-dicarboxylato – pyridyl coordination polymers and cell imaging with HepG2 cells.

Suprava Bhunia^a, Basudeb Dutta^a, Kunal Pal^b, Angeera Chandra^a, Kuladip Jana^b and Chittaranjan Sinha^{*a}

Sl. No.	Contents	Page No.
1.	IR spectroscopy of CP1 and CP1+Cu(II) ion.	2
2.	IR spectroscopy of CP2 and CP2+Cu(II) ion.	2
3.	Crystallographic data of CP1 (Table S2).	3
4.	Bond lengths and bond angles in CP1 (Table S3).	3,4
5.	Crystallographic data of CP2 (Table S4).	4,5
6.	Bond lengths and bond angles in CP2 (Table S5).	5
7.	List of H-bonding and spell field model of CP1.	6
8.	List of $\pi\cdots\pi$ stacking and spell field model of CP2.	6
9.	Powder X-ray Diffraction analysis of CP1 and CP2.	7
10.	Thermogravimetric analysis (TGA) of CP1 and CP2.	8
11.	UV Visible spectrum of CP1 and CP1+Cu(II) ion in water.	9
12.	UV Visible spectrum of CP2 and CP2+Cu(II) ion in water.	10
13.	Intensity changes of CP1 and CP2 at different Cu salts.	11
14.	pH plot of CP1 and CP2.	12
15.	Stren-Volmer plot of CP1 and CP2.	13
16.	Life time plot of CP1 and CP2.	14
17.	Limit of detection (LOD) plot of CP1 and CP2.	15
18.	Interaction of Cu(II) with CP1 and CP2	16
19.	Comparison data for Cu ²⁺ ion sensor (Table S1).	17
20.	Reference.	18

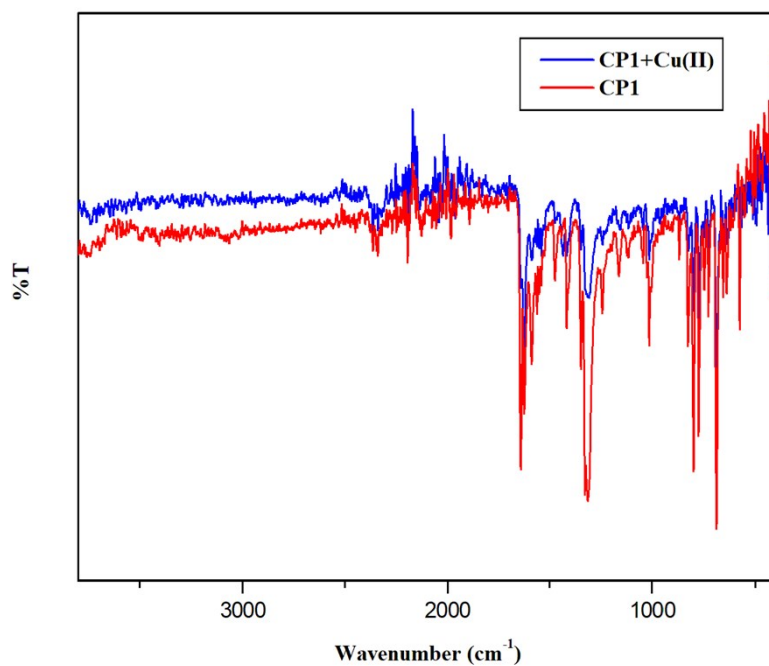


Figure S1. IR spectra of CP1 and CP1+Cu(II) ion.

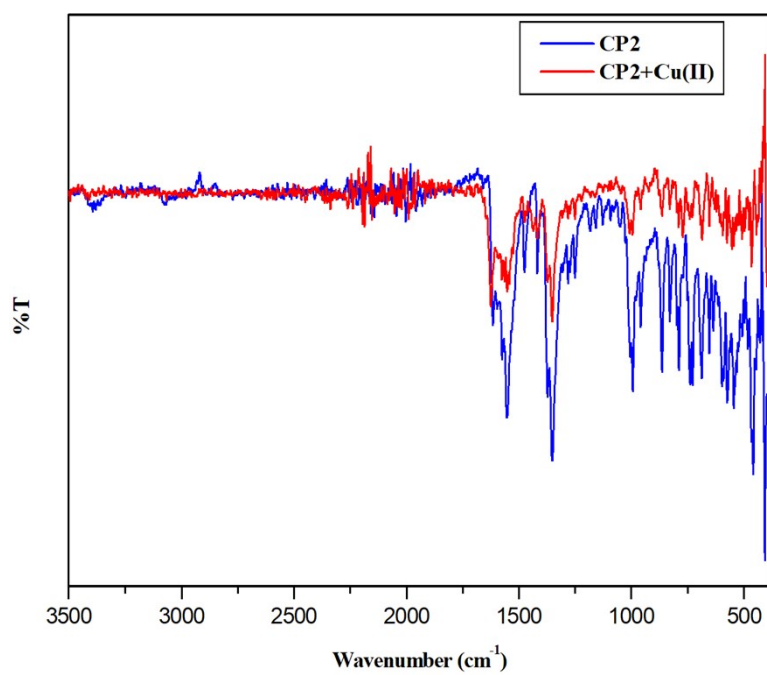


Figure S2. IR spectra of CP2 and CP2+Cu(II) ion.

Table S1 Crystal data and refinement parameters for compound CP1.

Formula	C ₁₉ H ₁₂ Cl N ₃ O ₅ Zn
fw	461.19
crystalsyst	triclinic
space group	<i>P</i> -1
<i>a</i> (Å)	9.0876(7)
<i>b</i> (Å)	10.0804(8)
<i>c</i> (Å)	11.7778(9)
α (deg)	66.626(2)
β (deg)	75.962(2)
γ (deg)	65.717(2)
<i>V</i> (Å ³)	898.68(12)
<i>Z</i>	2
<i>D</i> _{calcd} (g/cm ³)	1.704
μ (mm ⁻¹)	1.515
λ (Å)	0.71073
data[<i>I</i> > 2 σ (<i>I</i>)]/params	3093/268
GOF on <i>F</i> ²	1.343
final <i>R</i> indices[<i>I</i> > 2 σ (<i>I</i>)] ^{a,b}	<i>R</i> 1 = 0.0270 <i>wR</i> 2 = 0.0990

$$^a R1 = \frac{\sum ||F_o| - |F_c||}{\sum |F_o|}, \quad ^b wR2 = \left[\frac{\sum w(F_o^2 - F_c^2)^2}{\sum w(F_o^2)^2} \right]^{1/2}$$

Table S2 Selected bond lengths and bond angles in CP1.

Zn(1) - O(1)	1.9870(19)	N(1) - Zn(1) - O(4)b	87.32(8)
Zn(1) - O(3)	2.082(2)	N(2) - Zn(1) - N(3)	75.55(8)
Zn(1) - N(1)	2.154(2)	N(2) - Zn(1) - O(4)b	82.66(7)
Zn(1) - N(2)	2.080(2)	N(3) - Zn(1) - O(4)b	86.46(8)
Zn(1) - N(3)	2.166(2)	Zn(1) - O(3) - C(1)	120.03(17)
Zn(1) - O(4)b	2.510(2)	C(4) - O(4) - Zn(1)a	122.45(18)
O(1) - Zn(1) - O(3)	100.39(8)	Zn(1) - N(1) - C(15)	115.47(17)
O(1) - Zn(1) - N(1)	110.65(8)	Zn(1) - N(1) - C(19)	125.85(16)

O(1) - Zn(1) - N(2)	163.19(8)	Zn(1) - N(2) - C(10)	119.84(16)
O(1) - Zn(1) - N(3)	95.85(8)	Zn(1) - N(2) - C(14)	118.93(16)
O(1) - Zn(1) - O(4)b	82.41(7)	Zn(1) - N(3) - C(5)	124.97(16)
O(3) - Zn(1) - N(1)	95.18(8)	Zn(1) - N(3) - C(9)	115.85(17)
O(3) - Zn(1) - N(2)	94.03(7)	N(1) - Zn(1) - N(3)	151.69(7)
O(3) - Zn(1) - N(3)	89.46(8)	N(1) - Zn(1) - N(2)	76.27(8)
O(3) - Zn(1) - O(4)b	175.29(8)		

a = x, -1+y, z b = x, 1+y, z

Table S3 Crystal data and refinement parameters for compound CP2.

Formula	C ₂₁ H ₁₅ Cl N ₃ O ₅ Zn,
fw	490.20
crystalsyst	Triclinic
space group	<i>P</i> -1
<i>a</i> (Å)	8.697(5)
<i>b</i> (Å)	10.798(6)
<i>c</i> (Å)	13.165(7)
α (deg)	100.543(14)
β (deg)	105.004(14)
γ (deg)	113.587(14)
<i>V</i> (Å ³)	1035.5(10)
<i>Z</i>	2
<i>D</i> _{calcd} (g/cm ³)	1.572
μ (mm ⁻¹)	1.354
λ (Å)	0.71073
data[<i>I</i> > 2 σ (<i>I</i>)]/params	3529/286
GOF on <i>F</i> ²	1.073
final <i>R</i> indices[<i>I</i> > 2 σ (<i>I</i>)] ^{a,b}	<i>R</i> 1 = 0.0766 <i>wR</i> 2 = 0.2159

Table S4 Selected bond lengths and bond angles in CP2.

Zn(1) - O(1)	1.961(4)	N(1) - Zn(1) - N(2)	74.7(2)
Zn(1) - O(3)	1.951(5)	N(1) - Zn(1) - N(3)	150.69(18)
Zn(1) - N(1)	2.211(6)	N(2) - Zn(1) - N(3)	76.2(2)
Zn(1) - N(2)	2.092(5)	Zn(1) - O(1) - C(19)	119.5(4)
Zn(1) - N(3)	2.174(7)	Zn(1) - O(3) - C(3)	115.4(4)
O(1) - Zn(1) - O(3)	98.53(18)	Zn(1) - N(1) - C(14)	116.1(4)
O(1) - Zn(1) - N(1)	92.3(2)	Zn(1) - N(1) - C(18)	125.6(4)
O(1) - Zn(1) - N(2)	132.83(19)	Zn(1) - N(2) - C(9)	117.8(4)
O(1) - Zn(1) - N(3)	104.9(2)	Zn(1) - N(2) - C(13)	119.9(4)
O(3) - Zn(1) - N(1)	105.0(2)	Zn(1) - N(3) - C(4)	126.3(5)
O(3) - Zn(1) - N(2)	128.6(2)	Zn(1) - N(3) - C(8)	115.4(5)
O(3) - Zn(1) - N(3)	95.8(2)	N(1) - Zn(1) - N(3)	150.69(18)

a = x,-1+y,z

b = x,1+y,z

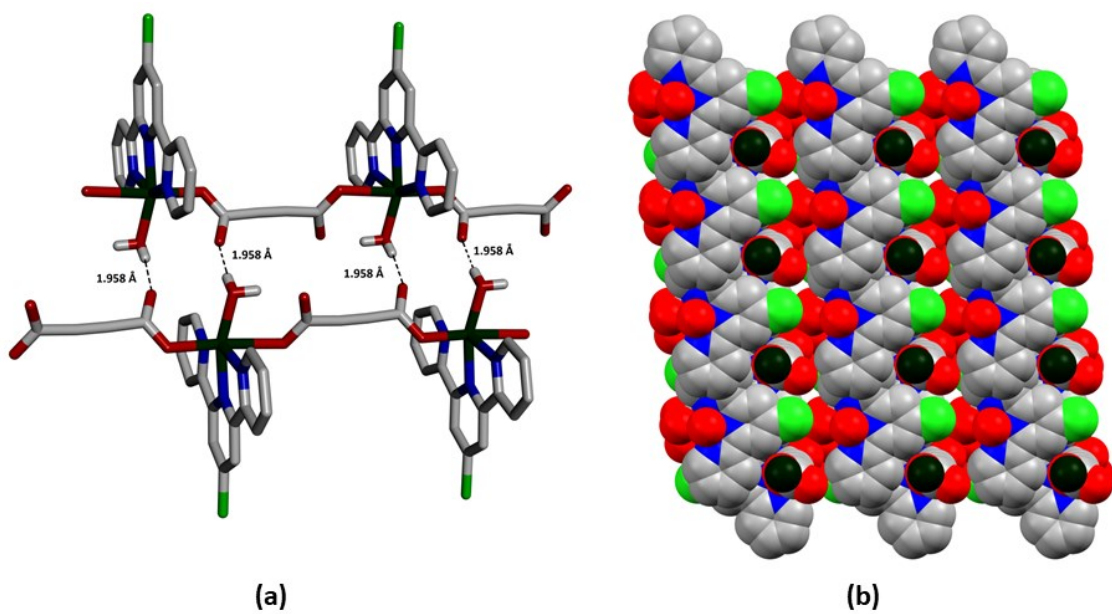


Figure S3. (a) H-bonding interaction between water and adc^{2-} ion in CP1. (b) spell field model of CP1.

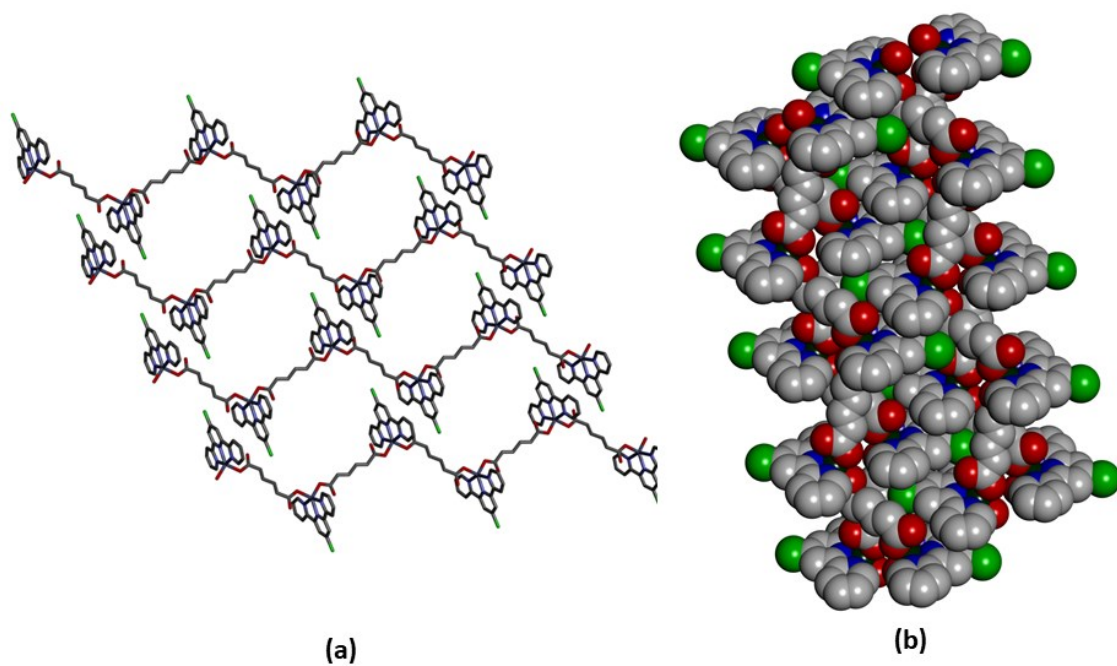


Figure S4. (a) Supramolecular aggregate of 1D coordination polymer. (b) Spell field model of CP2.

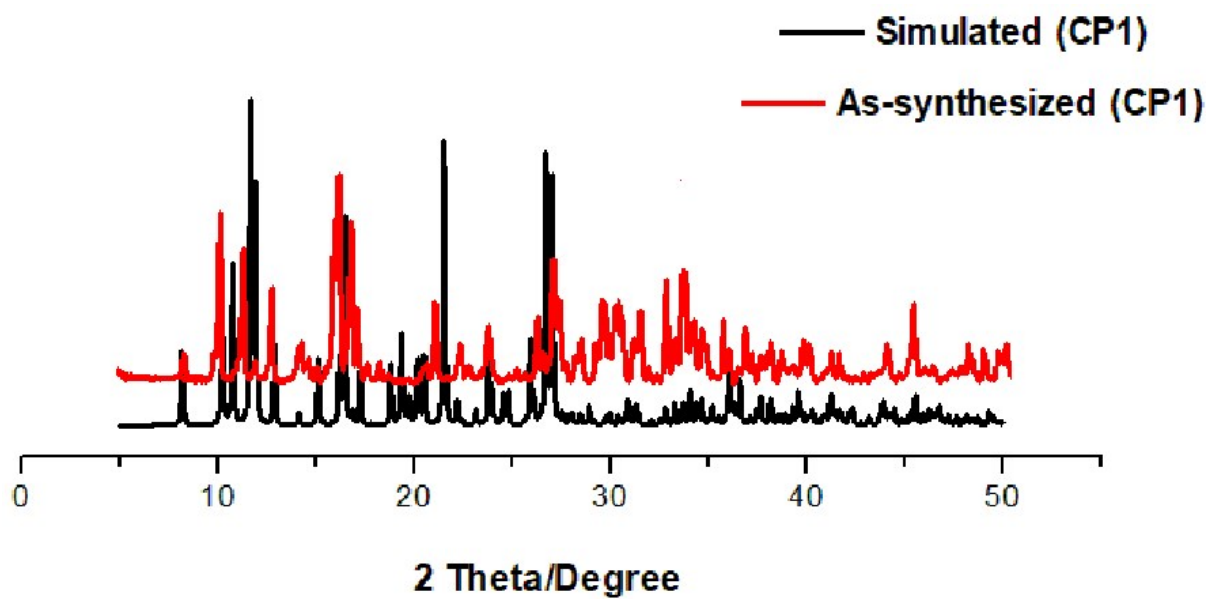


Figure S5. Powder X-ray Diffraction analysis of CP1.

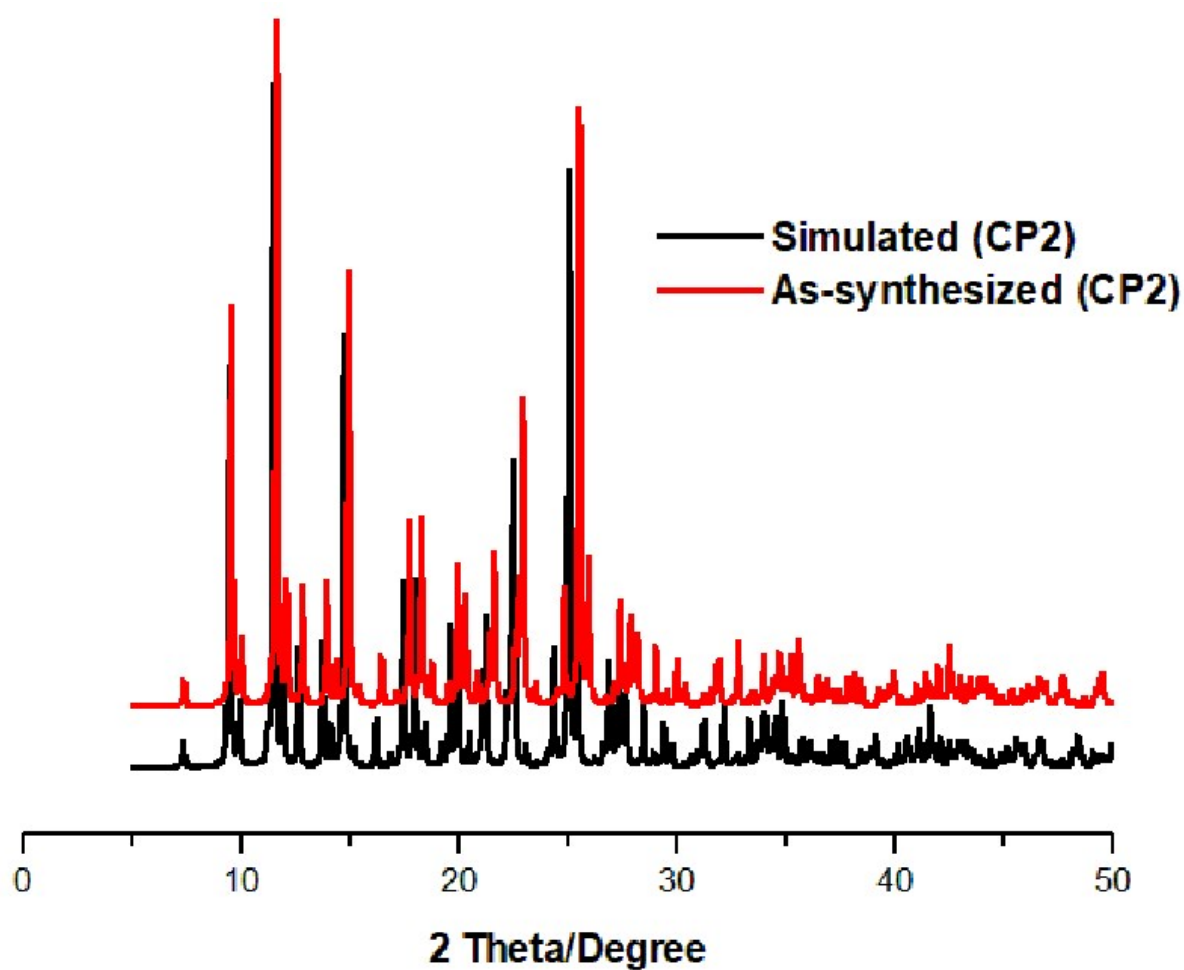


Figure S6. Powder X-ray Diffraction analysis of CP2.

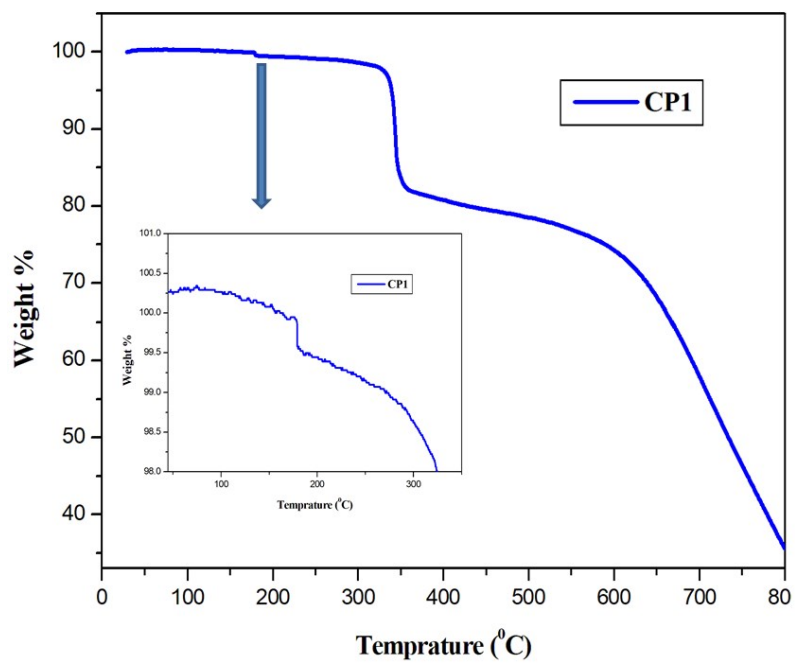


Figure S7. Thermogravimetric analysis (TGA) of CP1.

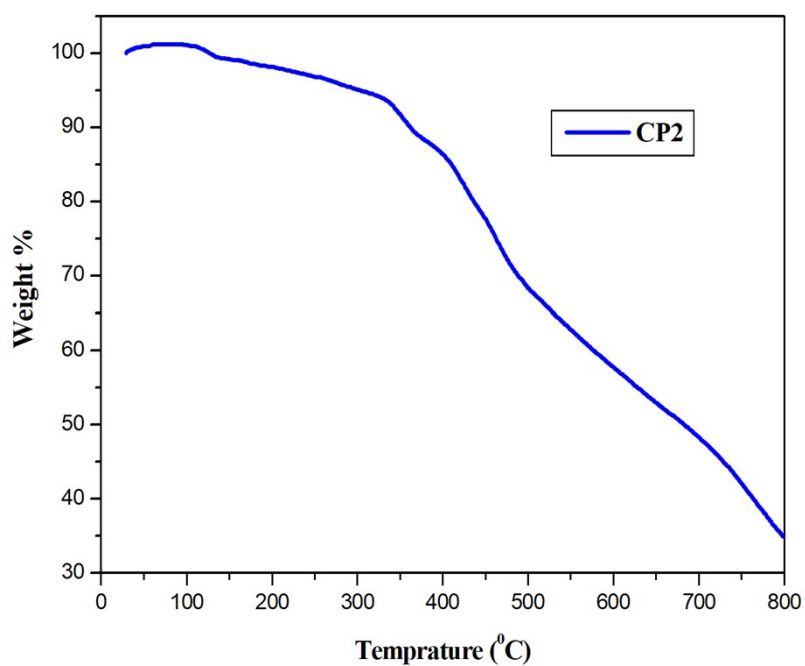
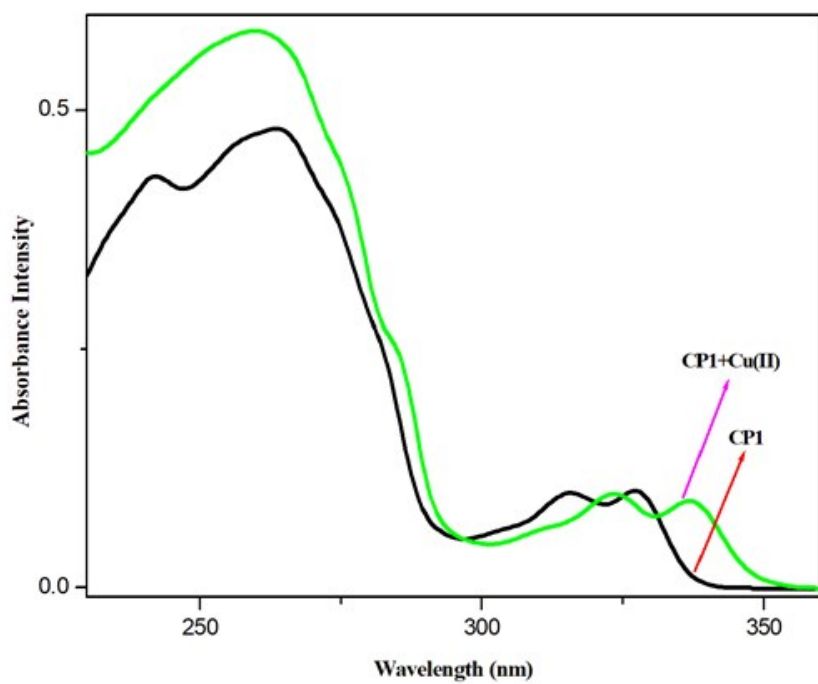
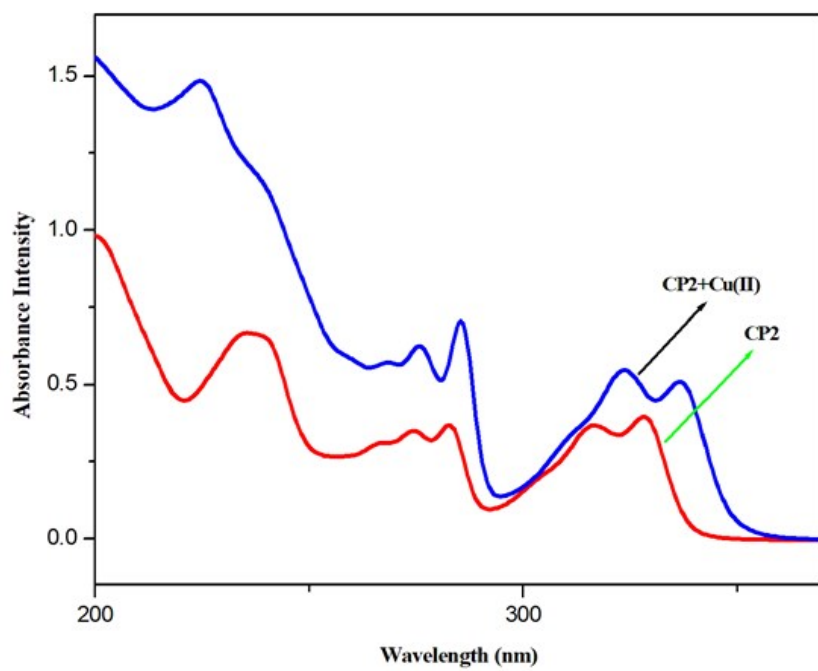


Figure S8. Thermogravimetric analysis (TGA) of CP2.



(a)

Figure S9. UV Visible spectrum of CP1 and CP1+Cu(II) in aqueous medium.



(b)

Figure S10. UV Visible spectrum of CP2 and CP2+Cu(II) in aqueous medium.

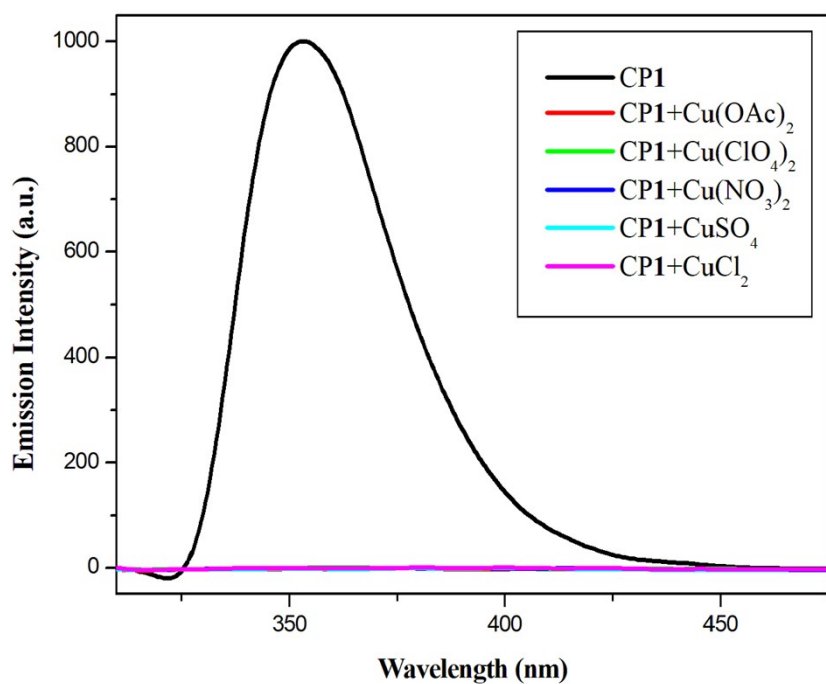


Figure S11. Emission Intensity of CP1 in presence of different Cu salts.

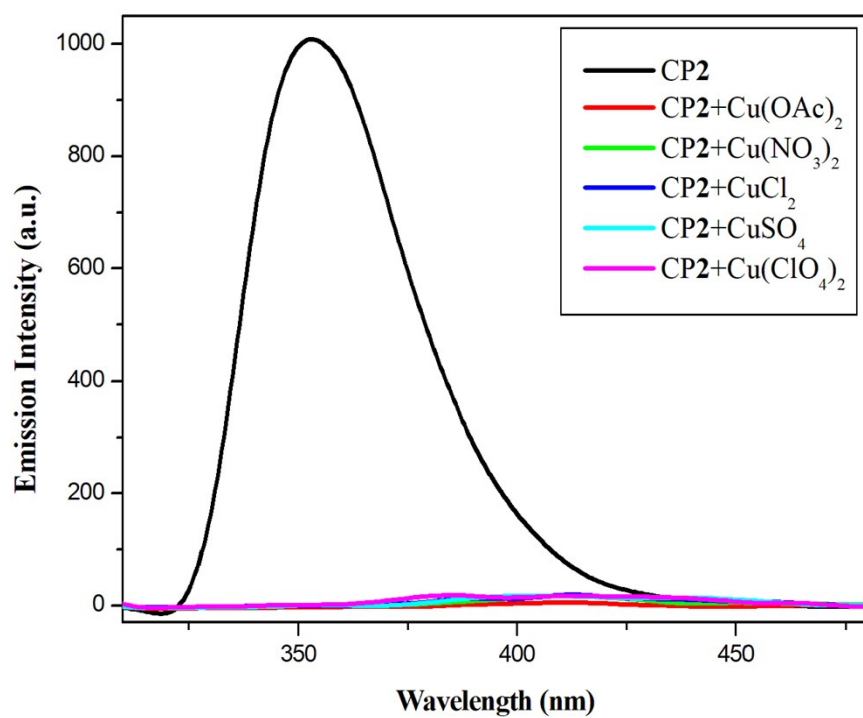


Figure S12. Emission Intensity of CP2 in presence of different Cu salts.

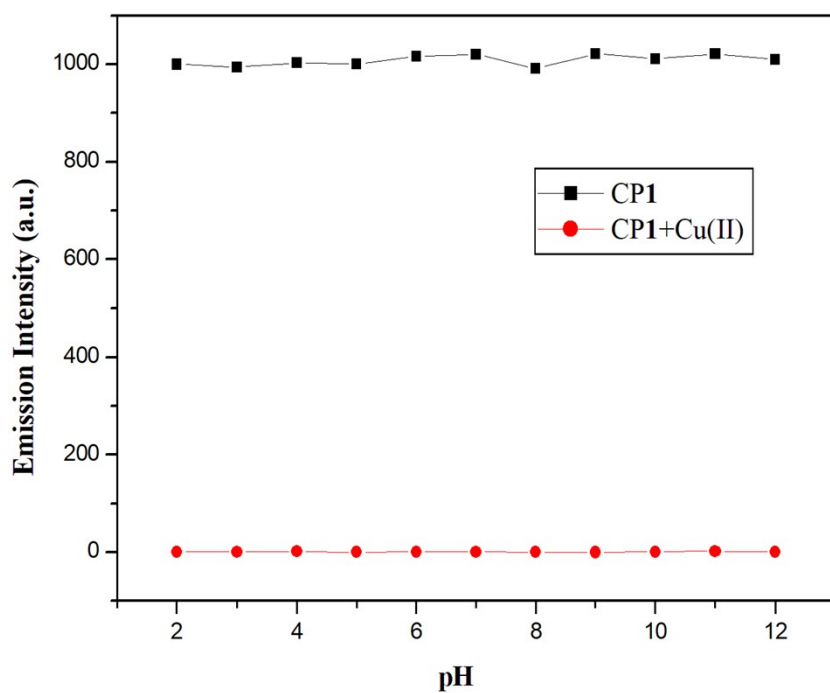


Figure S13. Emission Intensity of CP1 and CP1 in presence of Cu(II) ion at different pH.

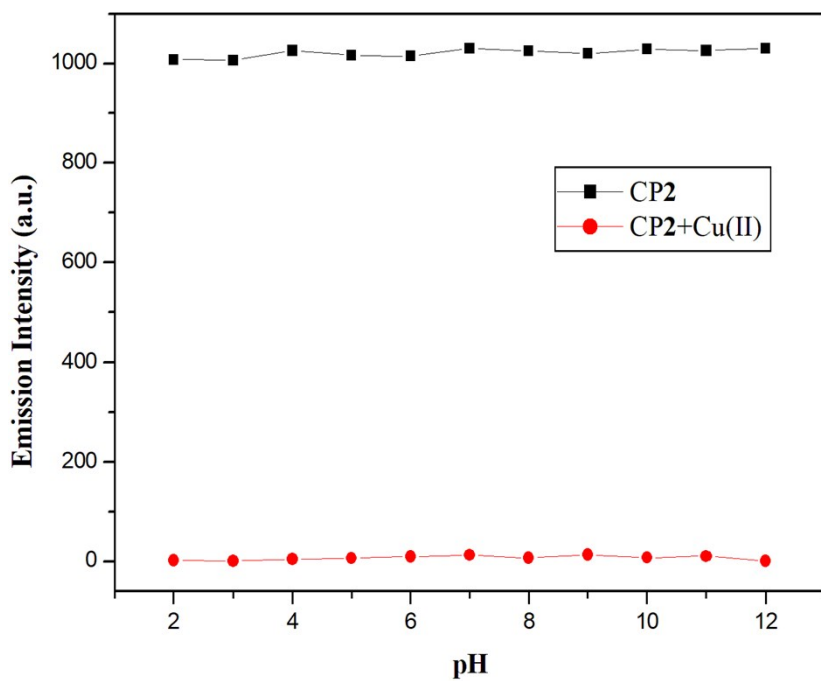


Figure S14. Emission Intensity of CP1 and CP1 in presence of Cu(II) ion at different pH.

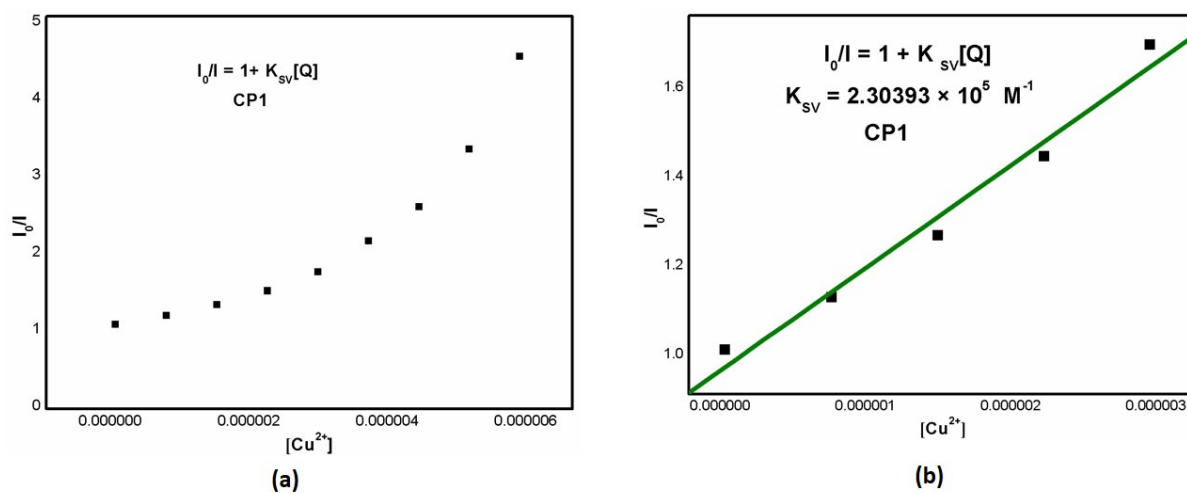


Figure S15. (a) Stern-Volmer plot of CP1. **(b)** Stern-Volmer plot of CP1 at lower range of quencher $[Cu^{2+}]$ (in M) concentration.

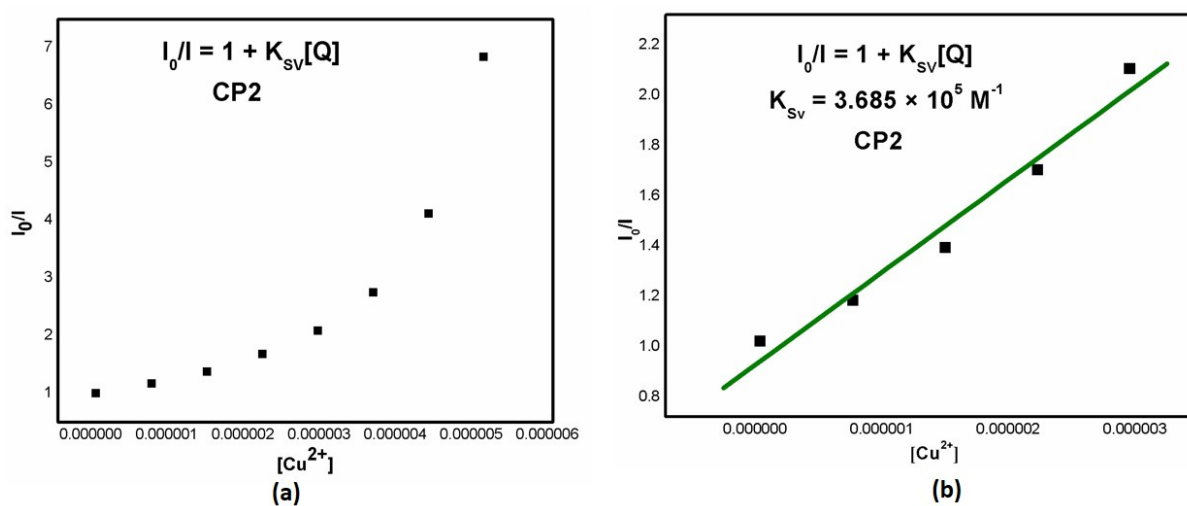


Figure S16. (a) Stern-Volmer plot of CP2. **(b)** Stern-Volmer plot of CP2 at lower range of quencher $[Cu^{2+}]$ (in M) concentration.

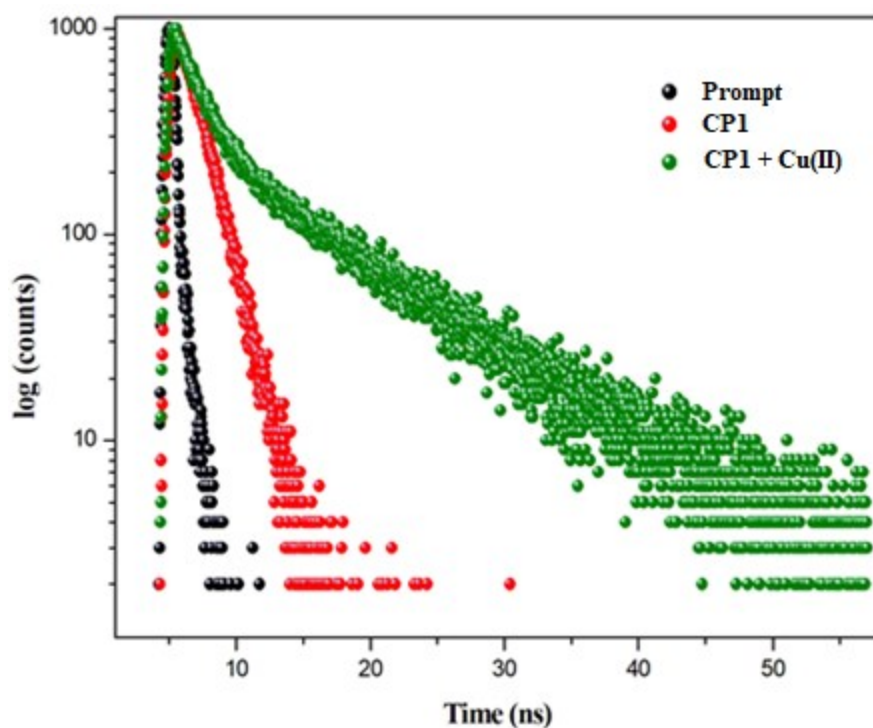


Figure 17 Excited state decay profile of prompt, CP1 and Cu^{2+} ion with CP1 in aqueous medium.

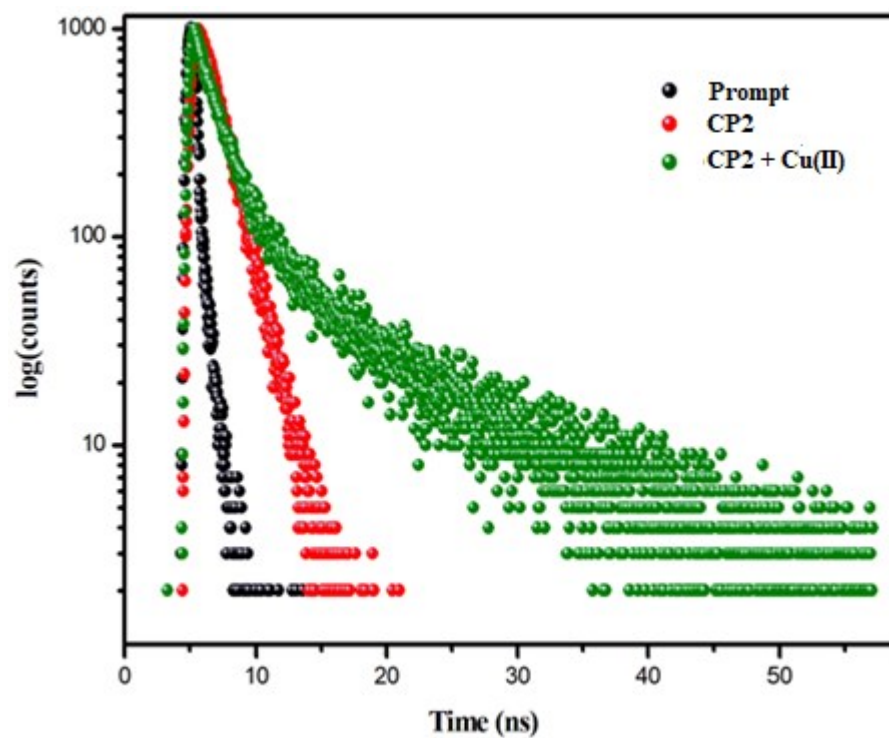


Figure S18 Excited state decay profile of prompt, CP1 and Cu^{2+} ion with CP1 in aqueous medium.

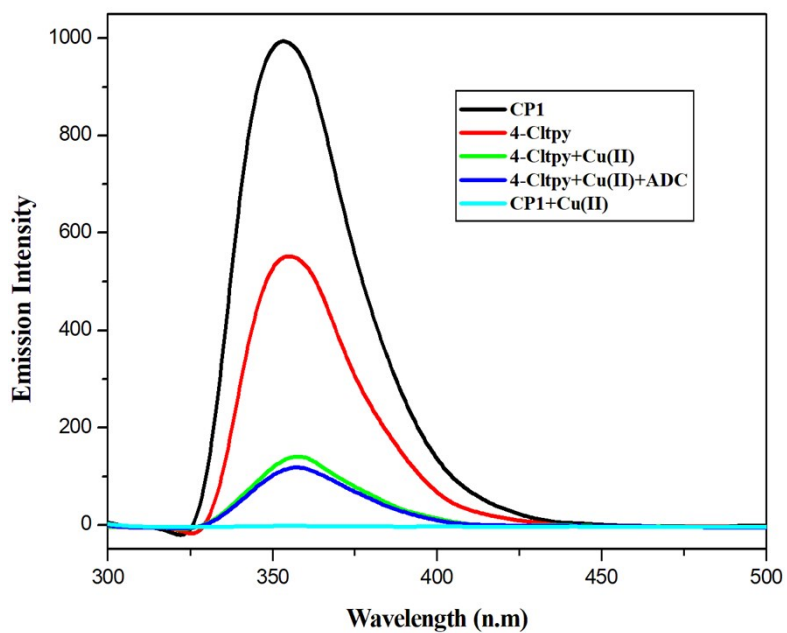


Figure S19 Emission intensity of CP1 , constitute materials of CP1 and their intensity change in presence of Cu(II) ion.

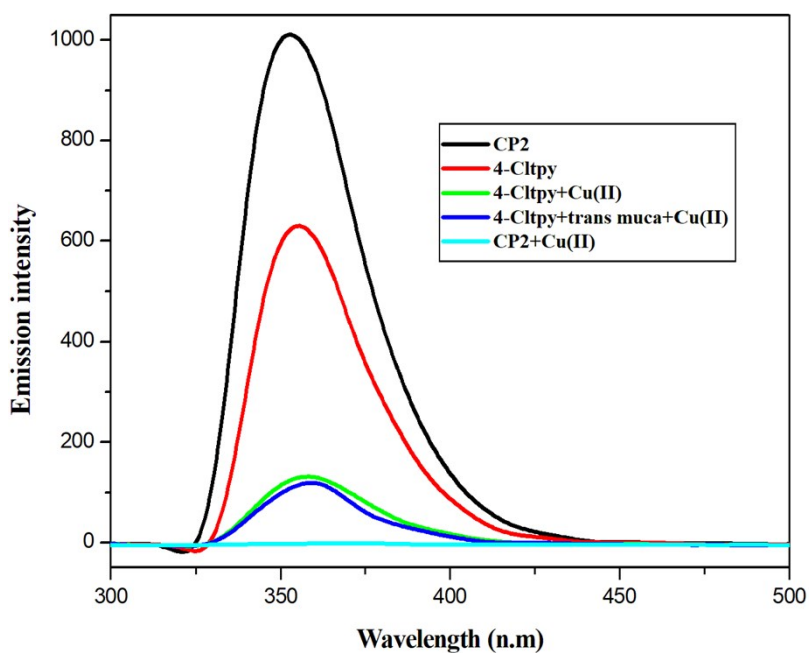


Figure S20 Emission intensity of CP2 , constitute materials of CP2 and their intensity change in presence of Cu(II) ion.

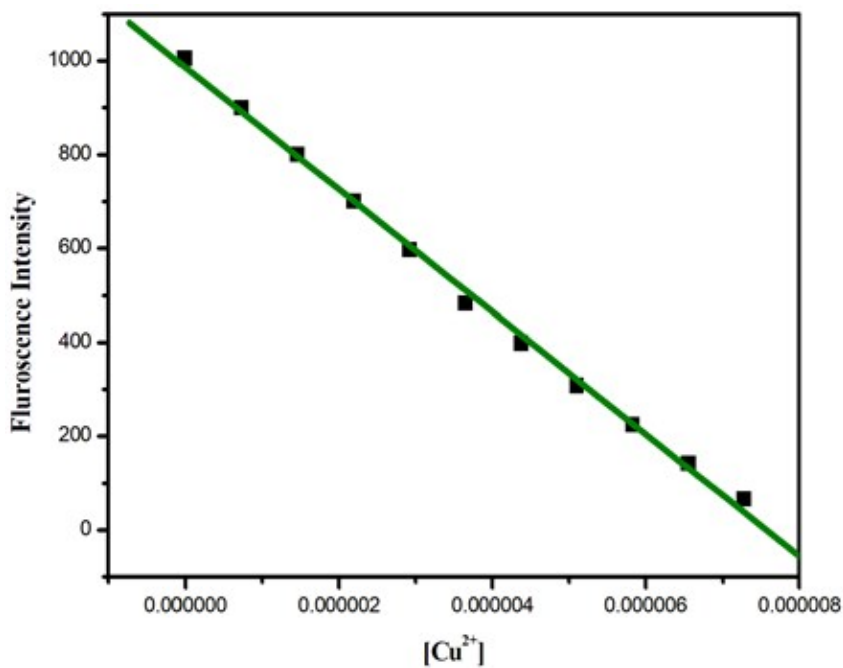


Figure S21 The linear dynamic response of CP1 for Cu²⁺ ion and the determination of the limit of detection(LOD) of Cu²⁺ ion.

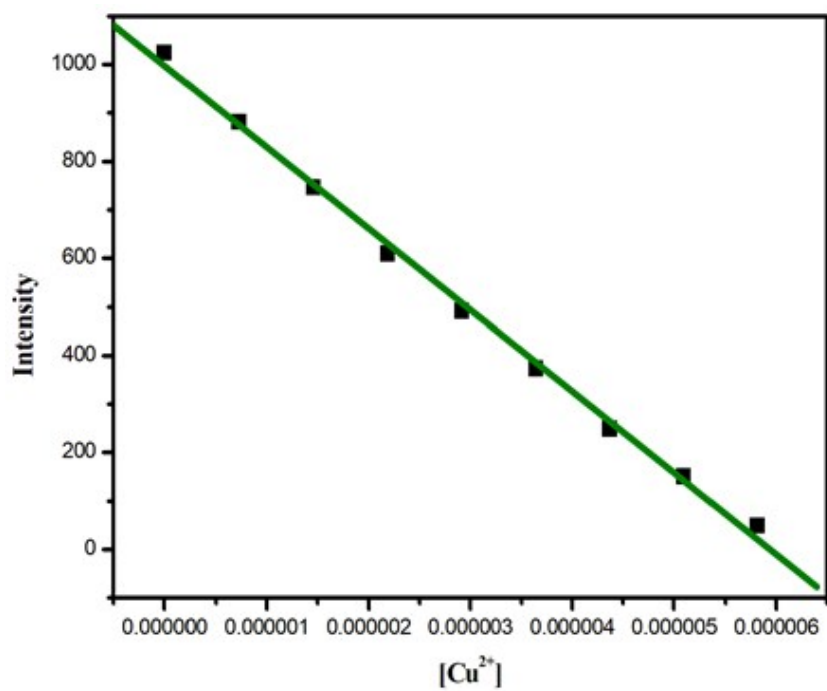


Figure S22 The linear dynamic response of CP2 for Cu²⁺ ion and the determination of the limit of detection (LOD) of Cu²⁺ ion.

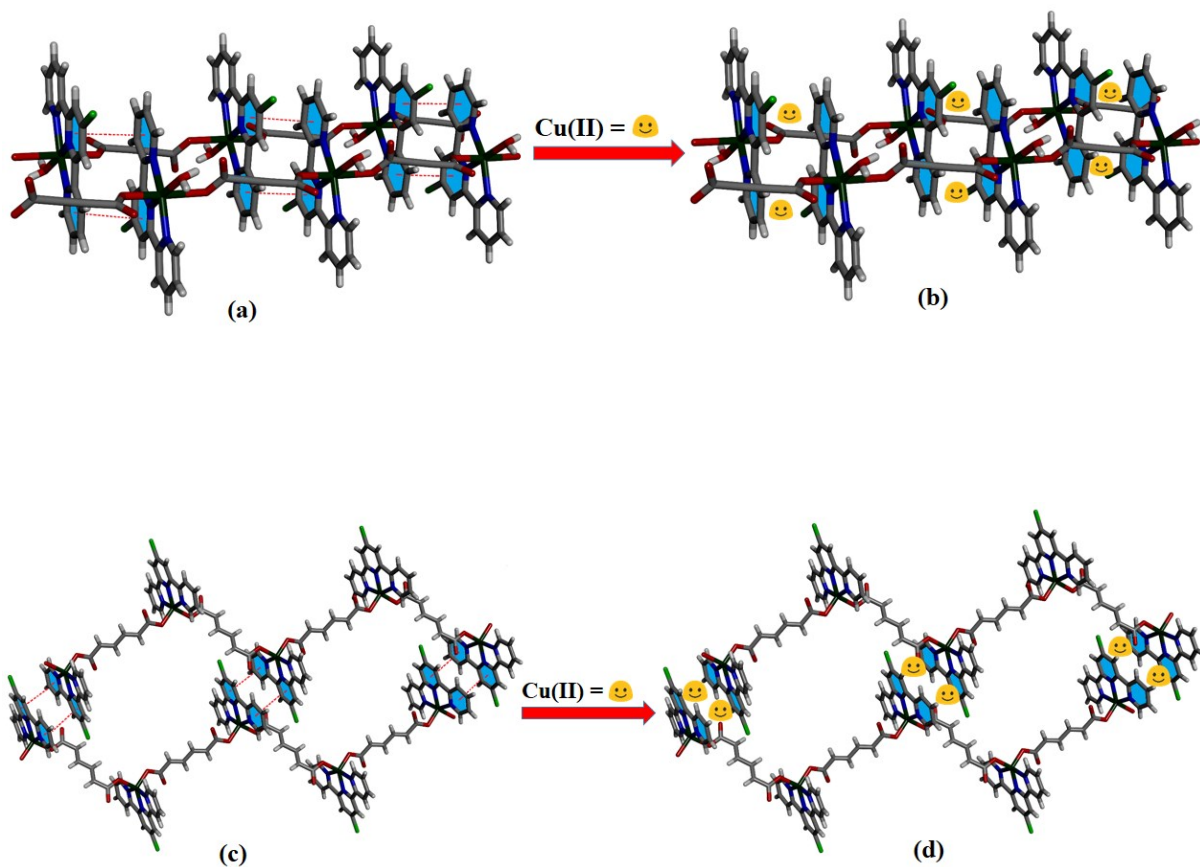
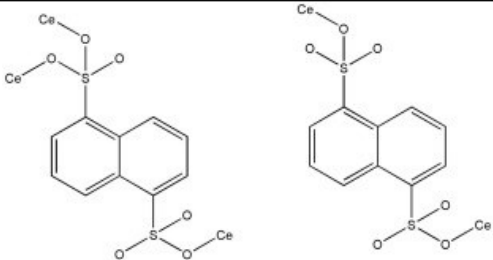
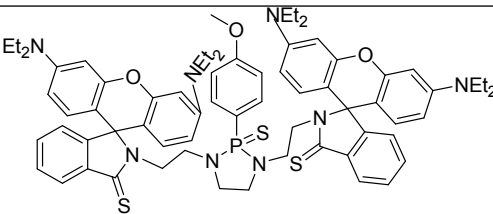
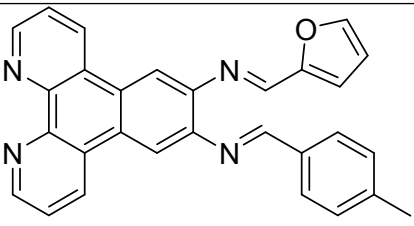


Figure S23. (a) $\pi \cdots \pi$ interaction between CP1 moiety, (b) interaction between Cu(II) and CP1, (c) $\pi \cdots \pi$ interaction between CP2 moiety, (d) interaction between Cu(II) and CP2.

Table S5 Comparison data for Cu²⁺ ion sensor.

Sl. No.	Ligand	Selectivity (LOD)	Solvent	Live Cell Imaging	Reference
1.		3.0 μM.	Water	No	1.
2.	SSA/AMP-Tb, 5-sulfosalicylic acid (SSA), adenosine monophosphate (AMP) and terbium ion (Tb ³⁺),	0.3 μM	HEPES buffer (0.1 M, pH 7.4)	No	2.
3.		0.01 μM.	MeCN	No	3.
4.		0.45 μM.	MeOH	No	4.
5.	CP1 and CP2	0.14 μM and 0.06 μM respectively.	Water	Yes	This Work

Reference:

1. S. Geranmayeh, M. Mohammadnejad and S. Mohammadi, *Ultrason. Sonochem.*, 2018, **40**, 453-459.
2. P. Huang, F. Wu and L.Mao, *Anal. Chem.* 2015, **87**, 6834-6841.
3. H. She, F. Song, J. Xu, X. Xiong, G. Chen,; J. Fan, S. Sun and X. Peng, *Chem. Asian J.* 2013, **8**, 2762-2767.
4. G. V. Vaidyanathan and U. B. Nair, *Dalton Trans.* 2012, **41**, 5769-5773.